Harmine hydrochloride induces G0/G1 cell cycle arrest and apoptosis in oral squamous carcinoma cells

WEITING LIN[1], YIZHEN LI[2], HSINYI HUANG[2], PEIWEN ZHAO[2], YINING SU[1] and CHIUNG-YAO FANG[2,3]

[1]Department of Stomatology, Ditmanson Medical Foundation Chiayi Christian Hospital, Chiayi 600, Taiwan, R.O.C.;
[2]Department of Medical Research, Ditmanson Medical Foundation Chiayi Christian Hospital, Chiayi 600, Taiwan, R.O.C.;
[3]Institute of Molecular Biology, National Chung Cheng University, Chiayi 621, Taiwan, R.O.C.

Received December 6, 2024; Accepted February 26, 2025

DOI: 10.3892/etm.2025.12861

Abstract. Oral squamous cell carcinoma (OSCC) represents the most frequently occurring form of oral cancer. However, despite the availability of advanced treatment modalities, the global 5-year survival rate for patients with advanced OSCC remains at ~50-60%. Devising alternative therapeutic strategies for oral cancer has therefore become an urgent need. Harmine, a β-carboline alkaloid, has recently been shown to exhibit anticancer activity. Compared with harmine, harmine hydrochloride (HH), a derivative of harmine, has improved water solubility and stability, so can absorb into tissues more readily. Therefore, the present study aimed to investigate the anticancer activity of HH in OSCC cells. A Cell Counting Kit-8 assay was performed to assess the cytotoxic effects of HH on the OSCC cell lines, SCC-4 and SCC-25. Flow cytometric analysis was subsequently employed to examine both the cell cycle profile and the extent of apoptosis. Western blotting was used to assess the expression levels of the regulatory proteins involved in these biological activities, and treatment with a pan-caspase inhibitor (Z-VAD-FMK) confirmed the involvement of the apoptotic pathway. Furthermore, western blotting was used to investigate which signaling pathways were affected in the HH-treated cells. Taken together, the findings of the present study demonstrated that HH was cytotoxic in OSCC cells. HH treatment induced G0/G1 phase cell cycle arrest and apoptosis. Additionally, the MAPK pathway was shown to be involved in HH-induced apoptosis in SCC-4 cells. Therefore, HH exhibited anticancer activity, and may be a putative therapeutic agent for the treatment of OSCC in the future.

Correspondence to: Dr Chiung-Yao Fang, Department of Medical Research, Ditmanson Medical Foundation Chiayi Christian Hospital, 539 Chung Hsiao Road, Chiayi 600, Taiwan, R.O.C.
E-mail: fcyo@ms72.hinet.net

Key words: harmine hydrochloride, oral squamous cell carcinoma, antitumor activity, apoptosis

Introduction

Oral cancer is a potentially fatal disease with a 5-year survival rate of 49.4%, and its incidence continues to increase by 2-3% per year (1,2). Furthermore, ~90% of all cases of oral cancer are histologically diagnosed as oral squamous cell carcinoma (OSCC) (3). The Global Cancer Observatory predicted a 40% increase in the incidence of OSCC by 2040, leading to a subsequent 0.6% rise in mortality rates (2,4). At present, surgical resection combined with radiotherapy or chemotherapy represents the primary therapeutic option for OSCC treatment (5,6). Neoadjuvant chemotherapy containing docetaxel, cisplatin and 5-fluorouracil (5-FU) remains the prominent adjuvant therapy for advanced oral cancers (7). However, drug resistance presents a formidable challenge when treating patients with OSCC (8); therefore, the development of novel drugs to improve the treatment of OSCC is urgently warranted.

Strategies for targeting molecular pathways in oral cancer cells have been intensively studied (9,10). The overexpression of EGFR, PI3K/Akt and mTOR has been identified in oral cancer tissues, and this increase in expression levels is associated with poor prognosis and survival rates (11,12); therefore, targeting these factors is a potentially promising strategy for oral cancer therapy (13,14). Alternatively, approaches to inhibiting VEGF signaling have been developed (15). These target therapies have provided encouraging results, increasing progression-free and overall survival in clinical trials (10,15); however, the heterogeneity of molecular pathways remains a challenge for oral cancer treatment.

Harmine is a β-carboline alkaloid with a diverse range of biological functions, including anti-inflammatory, anti-diabetic and anti-microbial activities, and it is isolated from the seeds of *Peganum harmala* L. (16,17). Harmine has been shown to be a potential herbal medicine effective against certain types of cancers, including bladder cancer, thyroid cancer and neuroblastoma (18,19), as harmine extracts have been reported to possess anticancer activity through inducing apoptosis, autophagy, targeting abnormal cell proliferation by regulating the cell cycle, angiogenesis and metastasis (20,21). Harmine hydrochloride (HH) is a harmine derivative that has improved stability compared with harmine and it is more easily absorbed by tissues (22). HH has been shown to exhibit anti-proliferative activity by inducing apoptosis, depleting the pools of cancer

stem cells and decreasing the rate of cell invasion by interfering with signaling pathways in gastric cancer, glioblastoma cells and hepatoma cell lines (17,22,23). However, to the best of our knowledge, the anti-proliferative activity of HH on OSCC cells has yet to be reported. The aim of the present study was to analyze the antiproliferation activity of HH and investigate the possible signaling pathways involved in HH-mediated cytotoxicity in oral cancer cells.

Materials and methods

Cell lines and cell culture. The human OSCC cell lines SCC-4 and SCC-25 were purchased from the Food Industry Research and Development Institute, and subsequently cultured following the instructions provided by the supplier. Specifically, SCC-4 cells were cultured in DMEM:F12 medium (cat. no. 11320033; Thermo Fisher Scientific, Inc.) containing 10% Gibco® FBS (cat. no. 104037028; Thermo Fisher Scientific, Inc.), 2 mM L-glutamine and 1% antibiotics (100 U/ml penicillin and 100 μg/ml streptomycin; cat. no. 15140122; Thermo Fisher Scientific, Inc.). SCC-25 cells were cultured in DMEM:F12 medium containing 10% FBS, 1.5 g/l sodium bicarbonate (cat. no. 25080094), 2.5 mM L-glutamine (cat. no. 25030081), 15 mM HEPES (cat. no. 15630-080) and 0.5 mM sodium pyruvate (cat. no. 11360070; all from Thermo Fisher Scientific, Inc.), with the additional provision of 400 ng/ml hydrocortisone (cat. no. H0888; Millipore Sigma). All the other supplements for cell cultures, with the exception of hydrocortisone, were obtained from Thermo Fisher Scientific, Inc. Cells were cultured in a humidified atmosphere containing 5% CO_2 at 37˚C and tested to ensure that they were free of mycoplasma contamination.

Reagents and antibodies. HH (cat. no. SMB00461) was purchased from Millipore Sigma. The protein extraction buffer, M-PER (cat. no. 78501; Thermo Fisher Scientific, Inc.), was used to lyse and extract proteins for subsequent western blotting analyses. The protease inhibitor cocktail (cat. no. 5971, 0.1%). was purchased from Cell Signaling Technology Inc. A 5 mM concentration of pan-caspase inhibitor Z-VAD-FMK (cat. no. V116; Millipore Sigma) was used to verify the apoptotic pathway. A 5 mM concentration of Rhodamine 123 (cat. no. R8004; Millipore Sigma) was used to detect the mitochondrial membrane potential (MMP). A 20 mM concentration of PD98059 (cat. no. 513000; Millipore Sigma), 20 mM of SP600125 (cat. no. 4420119; Millipore Sigma) and 10 mM of SB203580 (cat. no. 559389; Millipore Sigma) were used to inhibit signaling pathways in OSCC cells. The primary antibodies for the detection of apoptosis, namely the anti-caspase-3 (cat. no. 9662, 1:1,000), anti-caspase-8 (cat. no. 9746, 1:1,000), anti-caspase-9 (cat. no. 9502, 1:1,000), anti-poly (ADP-ribose) polymerase (anti-PARP) (cat. no. 9542, 1:1,000) and Bcl-xL (cat. no. 2764, 1:1,000) antibodies, were sourced from Cell Signaling Technology, Inc. The primary antibodies for the verification of cell cycle arrest, namely anti-CDK6 (cat. no. 13331, 1:1,000), anti-cyclin E2 (cat. no. 4132, 1:1,000), anti-p21 (cat. no. 2947, 1:1,000) and anti-p27 (cat. no. 2552, 1:1,000) antibodies, were purchased from Cell Signaling Technology, Inc. The primary antibodies for the signaling pathways, including p-ERK (cat. no. 4377, 1:1,000), ERK (cat. no. 4695, 1:1,000), p-AMPK (cat. no. 2531, 1:1,000), AMPK (cat. no. 2532, 1:1,000), p-MAPK9 (SAPK)/JNK (cat. no. 9251, 1:1,000), SAPK/JNK (cat. no. 9252, 1:1,000), p-MAPK (cat. no. 9215, 1:1,000) and MAPK (cat. no. 9212, 1:1,000) antibodies, were purchased from Cell Signaling Technologies, Inc. The expression level of GAPDH (cat. no. 2118, 1:5,000; Cell Signaling Technology, Inc.) was used as a loading control for western blotting analysis.

Cell viability analysis. The inhibition of growth activity of HH on the OSCC cells was evaluated using the Cell Counting Kit 8 (CCK-8) assay (cat. no. 96992; Millipore Sigma). Briefly, different concentrations of HH were applied to $1x10^4$ cells seeded in 96-well plates, followed by incubation for 24, 48 and 72 h at 37˚C in a humidified incubator. The CCK-8 reagent was added , and the absorbance was subsequently read at 490 nm after 2 h. The optical density (OD) of DMSO vehicle-treated cells (used as the control) was considered to be 100%. The OD values of HH-treated cells were divided by the value of control group, and the resulting ratios were considered to represent the survival rate of cells following HH treatment.

Clonogenic assay. The clonogenic assay measures the ability of a single cell to form a colony, defined as ≥50 cells. The clonogenic assays were performed to determine the long-term cytotoxicity of HH on OSCC cells. Briefly, $3x10^3$ cells were seeded in a 6-well plate. HH was added to the 6-well plate the next day. After 7 days of incubation, HH-treated or control OSCC cells were fixed with 10% formaldehyde for 30 min at 25˚C and visualized using 0.05% crystal violet (Millipore Sigma) staining for 15 min at 25˚C. ImageJ software (version 1.43, National Institutes of Health) was used to scan and analyze the colonies. The colony number of cells treated with the DMSO vehicle (control) was considered to be 100%. The colony numbers of HH-treated cells were divided by those of the control group, and the resulting ratios were considered to represent the rate of HH inhibition of oral cancer cell colony formation.

Cell cycle analysis. To determine whether HH treatment could affect the cell cycle profile of OSCC cells, $1x10^5$ cells were seeded in 6-well plates. Following 24 h of synchronization in a serum-free DMEM:F12 medium, cells were changed to 10% FBS DMEM:F12 medium and treated with HH for 12, 24, 36 and 48 h in a humidified atmosphere containing 5% CO_2 at 37˚C. A 100% methanol solution (cat. no. 34860; Millipore Sigma) was used to fix cells for 24 h at 4˚C. The DNA content was assessed by incubating the cells with 0.05 mg/ml propidium iodide (PI) (cat. no. 537060; Millipore Sigma) and 2 mg/ml RNase (cat. no. 11119915001; Roche Diagnostics) solution at 25˚C in the dark for 30 min, followed subsequently by flow cytometric analysis using the BD FACSCanto™ II (BD Biosciences) and the BD FACSDiva™ Software (version 6.0, BD Biosciences). The cell cycle profile was assessed using Modfit LT (version 3.3, Verity Software House) for cell cycle analysis. In brief, after staining cellular DNA with PI and analyzing the data using flow cytometric software, the results were further processed using ModFit analysis. This analysis produced fluorescence intensity graphs based on the DNA content, which allowed the identification of cell proportions

in the G0/G1, S and G2/M phases of the cell cycle, thereby determining how HH affects the cell cycle in oral cancer.

Flow cytometric analysis for the detection of apoptosis. The OSCC cells were treated with HH for 24 or 48 h in a humidified atmosphere containing 5% CO_2 at 37˚C. Apoptotic cells were subsequently stained with annexin V-FITC and PI using an apoptosis detection kit (cat. no. K101-100; BioVision, Inc.). During early apoptosis, the inner cell membrane flips outwards, exposing phosphatidylserine, which is able to bind to annexin V-FITC. PI is a DNA intercalating dye that is able to enter the nucleus of cells with damaged membranes (22). The fluorescence intensities of annexin V-FITC and PI were detected by flow cytometry using the BD FACSCanto™ II (BD Biosciences) and BD FACSDiva™ software (version 6.0, BD Biosciences). The apoptotic cell ratio was calculated as the sum of early apoptosis (FITC fluorescence only) and late apoptosis (where both FITC and PI fluorescence were detected).

Flow cytometric analysis for the detection of MMP. A total of $1x10^5$ cells OSCC cells were treated with HH for 24 or 48 h in 6-well plates in a humidified atmosphere containing 5% CO_2 at 37˚C. After treatment, the cells were detached using 0.25% Trypsin-EDTA (cat. no. 25200056, Thermo Fisher Scientific, Inc.), washed with PBS and stained with 5 μM Rhodamine 123 (Millipore Sigma) at 37˚C for 30 min. After staining, the cells were washed with PBS and analyzed by flow cytometry using the BD FACSCanto™ II (BD Biosciences) and BD FACSDiva™ software (version 6.0, BD Biosciences).

Cell lysate preparation and western blotting. The proteins of HH-treated SCC-4 and SCC-25 cells were lysed and extracted using M-PER mammalian protein extraction containing a 0.1% protease inhibitor cocktail (cat. no. 7012; Cell Signaling Technology, Inc.). The protein concentration was determined using the Bio-Rad Protein Assay reagent (cat. no. 5000001; Bio-Rad Laboratories, Inc.). SDS-PAGE, using a 12.5% gel, was performed to separate 40 μg of each sample, followed by transfer on to a PVDF membrane (cat. no. 1620177; Bio-Rad Laboratories, Inc.). The membrane was blocked in 5% bovine serum albumin (cat. no. A2153, MilliporeSigma) at 25˚C for 1 h. The membrane was probed with the primary specific antibodies in 5% BSA (cat. no. A2153, MilliporeSigma) as indicated in the reagent and antibodies section at 4˚C for 16 h. Subsequently, the membrane was incubated with horseradish peroxidase-conjugated secondary antibodies (anti-mouse, cat. no. AB_10015289; anti-rabbit, cat. no. AB_2337936; both purchased from Jackson ImmunoResearch Laboratories, Inc.) at 25˚C for 2 h. Protein expression was detected using an enhanced chemiluminescence horseradish peroxidase substrate detection kit (cat. no. WBKLS0500; Millipore Sigma). Finally, quantification of protein expression was performed by analyzing the densities of the gray bands using a UVP BioSpectrum 800 Imaging System.

Migration and invasion assay. For the migration assay, $2x10^5$ OSCC cells in 200 μl serum-free DMEM:F12 medium were seeded in the upper chamber of 8 μm cell culture inserts (cat. no. PI8P01250; Millipore Sigma), and 10, 15 or 20 μM of HH for SCC-4 cells and 5, 10 or 15 μM of HH for SCC-25 cells were added. For cell migration experiments, DMEM:F12 medium containing 20% FBS was added to the lower chamber, and the cells were incubated for 24 or 48 h in a humidified atmosphere containing 5% CO_2 at 37˚C. Following incubation, non-migrated cells in the upper chamber were carefully removed using a cotton swab. The migrated cells were fixed with 4% paraformaldehyde for 10 min at 25˚C, washed with PBS, subsequently stained with 0.2% crystal violet for 30 min at 25˚C. The excess dye was washed off using PBS samples were imaged using the IX83 inverted light microscope (Olympus Corporation). The fixed migrated cells were then counted using ImageJ software. For the invasion assay, the protocol followed was identical with that of the migration assay, except that 100 μl Matrigel™ (Corning, Inc.) diluted in serum-free DMEM:F12 medium at a concentration of 1:5 was added to the upper chamber and incubated at 37˚C for 2 h.

Statistical analysis. The results were analyzed for statistical significance using GraphPad Prism software (version 7.0; Dotmatics). One-way ANOVA followed by Bonferroni's post hoc multiple comparison test was used to analyze data. All *in vitro* experiments were performed in triplicate and data are shown as the mean ± SD. $P<0.05$ was considered to indicate a statistically significant difference.

Results

HH exhibits growth inhibitory activity in human OSCC cells. To assess whether HH exerts effective anti-growth activity on human OSCC cells, SCC-4 and SCC-25 cells were treated with HH, and the resulting cell survival rates were analyzed using CCK-8 and clonogenic assays. HH treatment was found to exert a cytotoxic effect on both SCC-4 and SCC-25 cells in a concentration- and time-dependent manner (Fig. 1A and B). The IC_{50} values were determined to be 41.73, 32.92 and 18.7 μM in SCC-4 cells, and 35.41, 13.52 and 12.38 μM in SCC-25 cells, after 24, 48 and 72 h of treatment with HH, respectively. A clonogenic assay was further used to determine the long-term cytotoxicity of HH on OSCC cells. The number of colonies was reduced in a concentration-dependent manner following HH treatment. At a low concentration (5 μM), HH treatment of SCC-4 and SCC-25 cells resulted in a statistically significant reduction in colony formation ability. As the concentration increased to 10 μM, the number of colonies of SCC-4 and SCC-25 cells decreased to <50% of the control group. At the highest concentration (15 μM), colony formation was reduced to ~10% of the control group (Fig. 1C and D). Taken together, these data suggested that HH treatment may exert an inhibitory effect on human OSCC cell proliferation.

HH causes cell cycle arrest at the G0/G1 phase. To analyze the underlying mechanisms via which HH inhibits the growth of OSCC cells, flow cytometric analysis was performed to determine the cell cycle distribution profiles following HH treatment. After HH treatment of SCC-4 and SCC-25 cells for 12, 24, 36 and 48 h, the cell cycle was found to have been arrested at the G0/G1 phase in a concentration-dependent manner (Figs. 2A and S1). Furthermore, the expression levels of cell cycle marker proteins were determined using western blotting. CDK6 performs its role in conjunction with CDK4

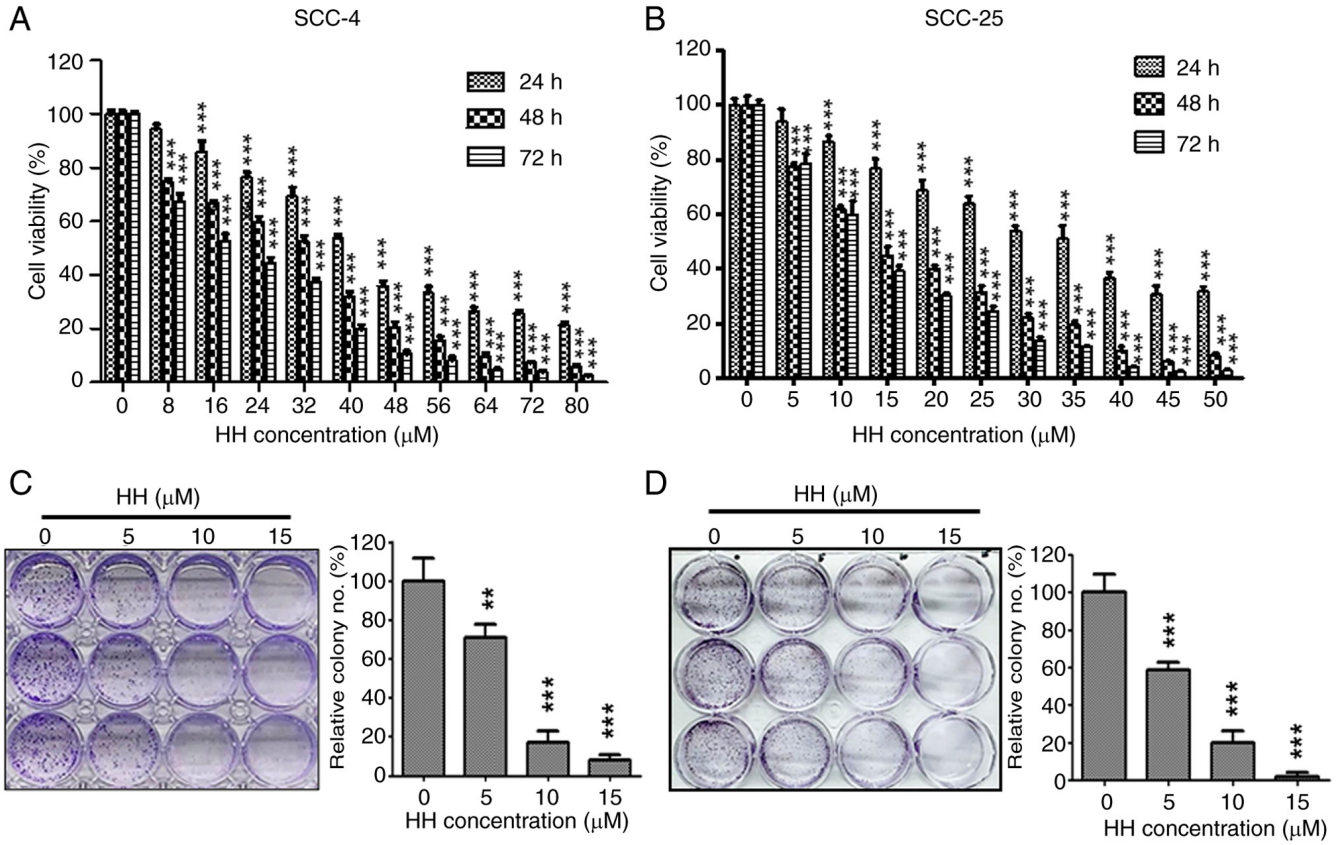

Figure 1. Cytotoxicity of HH on oral cancer cells. (A) SCC-4 cells were treated with the indicated concentration of HH for 24, 48 and 72 h and cell viability was assessed using the Cell Counting Kit-8 assay. In SCC-4 cells treated with HH, cell viability was significantly reduced compared with the control group (HH 0 μM) at 16 μM following 24 h and at 8 μM following 48 or 72 h. (B) SCC-25 cells were treated with the indicated concentration of HH for 24, 48 and 72 h and cell viability was assessed using the Cell Counting Kit-8 assay. In SCC-25 cells treated with HH, cell viability was significantly reduced compared with the control group (HH 0 μM) at 10 μM following 24 h and at 5 μM following 48 or 72 h. (C) SCC-4 and (D) SCC-25 cells were treated with HH for 7 days and the colony formation capacity of cell was assessed. Colonies were quantified using ImageJ software (version 1.43, National Institutes of Health). HH 0 μM represents DMSO as the solvent for dissolving HH and serves as the control group. Data are presented as mean ± SD (n=3). **P<0.01 and ***P<0.001. HH, harmine hydrochloride.

to facilitate cell cycle progression from the G1 phase to the S phase (24,25). Cyclin E2 performs a supportive role in a rate-limiting step for G1 progression (26). Furthermore, the proteins p21 and p27 are known to bind to CDKs and to inhibit cell cycle progression (27,28). The protein expression levels of CDK6 and cyclin E2 were decreased upon treatment with HH (Fig. 2B). By contrast, the protein expression levels of p21 and p27 increased. Taken together, the results of the flow cytometry and western blotting experiments suggested that HH treatment induced arrest of the SCC-4 and SCC-25 cells at the G0/G1 phase. Additionally, HH treatment increased the ratio of sub-G1 phase cells (Fig. S1). Furthermore, after treating SCC-4 cells with HH for 12, 24, 36 and 48 h, the number of subG1 cells significantly increased in a concentration- and time-dependent manner. This effect was particularly significant at the highest concentration of 45 μM. By contrast, when SCC-25 cells were treated with 15 μM HH, the subG1 ratio showed a slight increase at 12, 24, 36 and 48 h; however, this increase was not statistically significant. Treatment with 35 μM HH for 12 and 24 h resulted in a significant increase in the subG1 cell ratio compared with the controls. However, as the treatment duration increased, the subG1 cell ratio in SCC-25 cells decreased, and by 48 h, the difference was no longer statistically significant (Fig. 2C). Collectively, these results suggested that HH treatment induces G0/G1 cell cycle arrest and may subsequently trigger OSCC apoptosis.

HH induces apoptosis in OSCC cells. As aforementioned, HH treatment resulted in an increase in the population of sub-G1 cells in OSCC cells. The extent of apoptosis was further assessed in HH-treated OSCC cells using flow cytometric analysis with annexin V/PI double staining. Following HH treatment, annexin-V staining was significantly increased at all HH concentrations tested in the SCC-4 cells compared with the controls, suggesting the occurrence of apoptotic cell death (Fig. 3A and B). The expression levels of apoptosis-associated proteins were further determined using western blotting. The level of cleaved PARP was increased following HH treatment at 24 and 48 h (Fig. 3C). Moreover, increased cleaved/proform ratios of caspases-3, -8 and -9 were observed at 48 h upon treatment of the SCC-4 cells with a higher concentration of HH. By contrast, the expression level of the anti-apoptotic factor, Bcl-xL, was found to decrease (Fig. 3C). Taken together, these data suggested that intrinsic and extrinsic caspases may be involved in HH-induced apoptosis. Subsequently, changes in the MMP following HH treatment in SCC-4 cells were examined to confirm the involvement of the intrinsic caspase pathway. An observed increase in rhodamine 123 staining

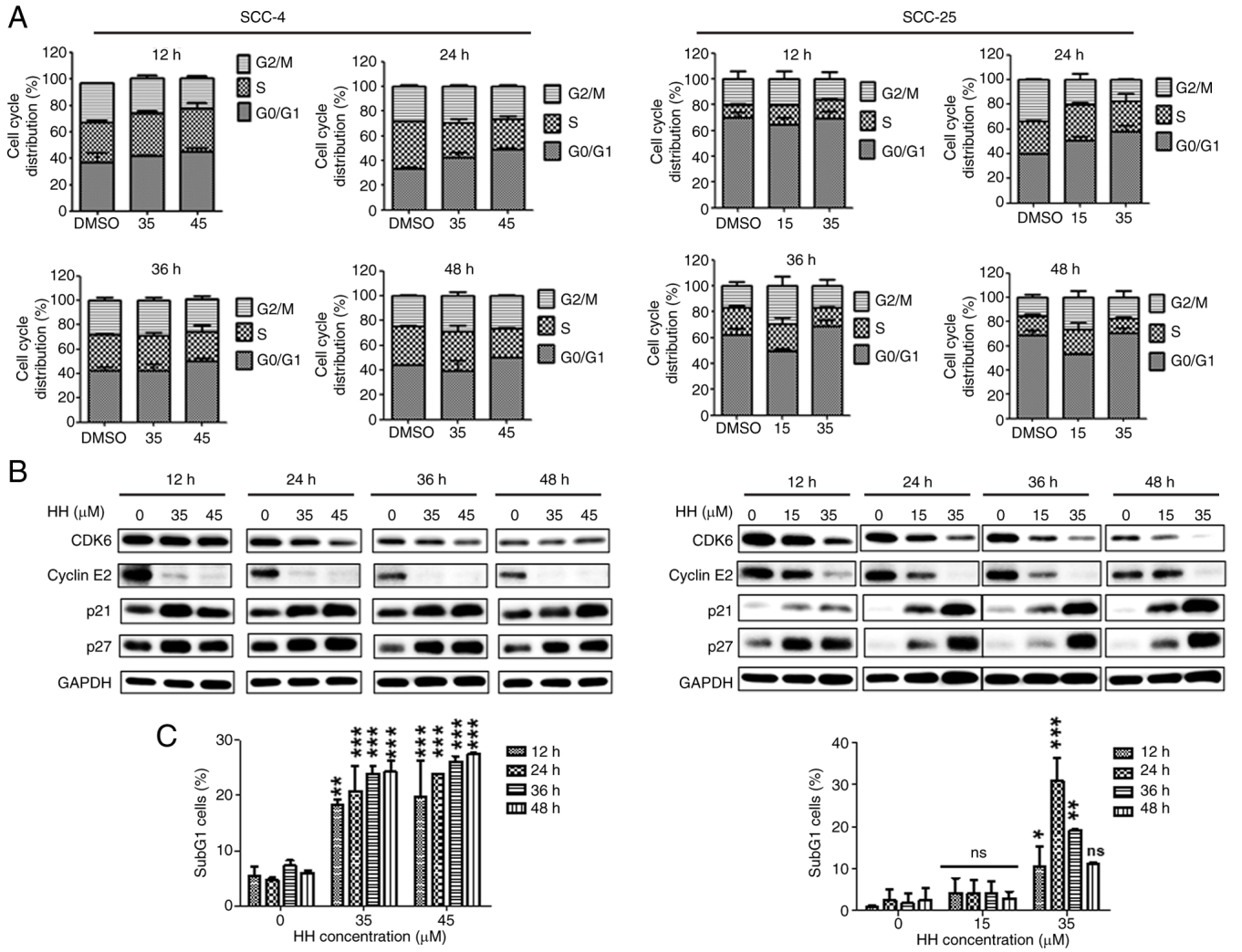

Figure 2. HH induces G0/G1 cell cycle arrest in oral cancer cells. (A) SCC-4 (left panel) and SCC-25 (right panel) cells were treated with the indicated concentrations of HH for 12, 24, 36 or 48 h, followed by cell cycle distribution analysis using flow cytometric analysis. (B) SCC-4 (left panel) and SCC-25 (right panel) cell cycle regulation protein expression was assessed using western blotting analysis. (C) The proportion of sub-G1 phase cells after HH treatment is shown. HH 0 μM represents DMSO as the solvent for dissolving HH and serves as the control group. Data are presented as mean ± SD (n=3). *P<0.05, **P<0.01, ***P<0.01 vs. control. HH, harmine hydrochloride; ns, not significant.

was indicative of a loss of MMP, which showed a significant increase with increased HH treatment concentration and duration. At 24 h, the cells treated with 45 μM demonstrated an ~4X increase in rhodamine 123 compared with the control group, and this was significantly increased further at the 48 h, suggesting the involvement of the intrinsic caspase pathway in HH-triggered apoptosis in SCC-4 cells (Fig. 3D). Similarly, HH treatment increased the level of apoptosis in SCC-25 cells. Following HH treatment, annexin-V staining was significantly increased at all HH concentrations in SCC-25 cells. When cells were treated with a high concentration of 35 μM HH, apoptosis was ~4X higher compared with that of the control group, regardless of the treatment duration, suggesting the occurrence of apoptotic cell death in HH-treated SCC-25 cells (Fig. 4A and B). Subsequent western blotting analysis further confirmed increases in the protein expression levels of caspases-3, -8, -9 and cleaved PARP, with a concomitant decrease in the protein expression level of the anti-apoptotic factor, Bcl-xL, in HH-treated SCC-25 cells (Fig. 4C). Loss of MMP was further detected through the increase of rhodamine 123 staining in SCC-25 cells, which intensified with increased HH concentration and duration. At 24 h, 35 μM HH treatment increased rhodamine 123 staining ~4X compared with the control, which increased significantly at 48 h, suggesting intrinsic caspase pathway involvement in HH-induced apoptosis in SCC-25 cells (Fig. 4D). Taken together, these results demonstrated that HH treatment induced apoptosis in human SCC-4 and SCC-25 OSCC cells.

Caspases are involved in HH-induced apoptotic cell death in OSCC cells. Experiments were subsequently devised to further determine the involvement of caspases in HH-induced apoptosis in OSCC cells. A pan-caspase inhibitor, Z-VAD-FMK, was applied to OSCC cells prior to HH treatment. When SCC-4 cells were pretreated with Z-VAD-FMK before HH treatment, HH-mediated apoptosis was significantly attenuated in SCC-4 cells compared with cells that were not pretreated. (Figs. 5A and S2A). This result was further confirmed through the identification of decreased levels of apoptosis-associated proteins via western blotting, including the cleaved forms of

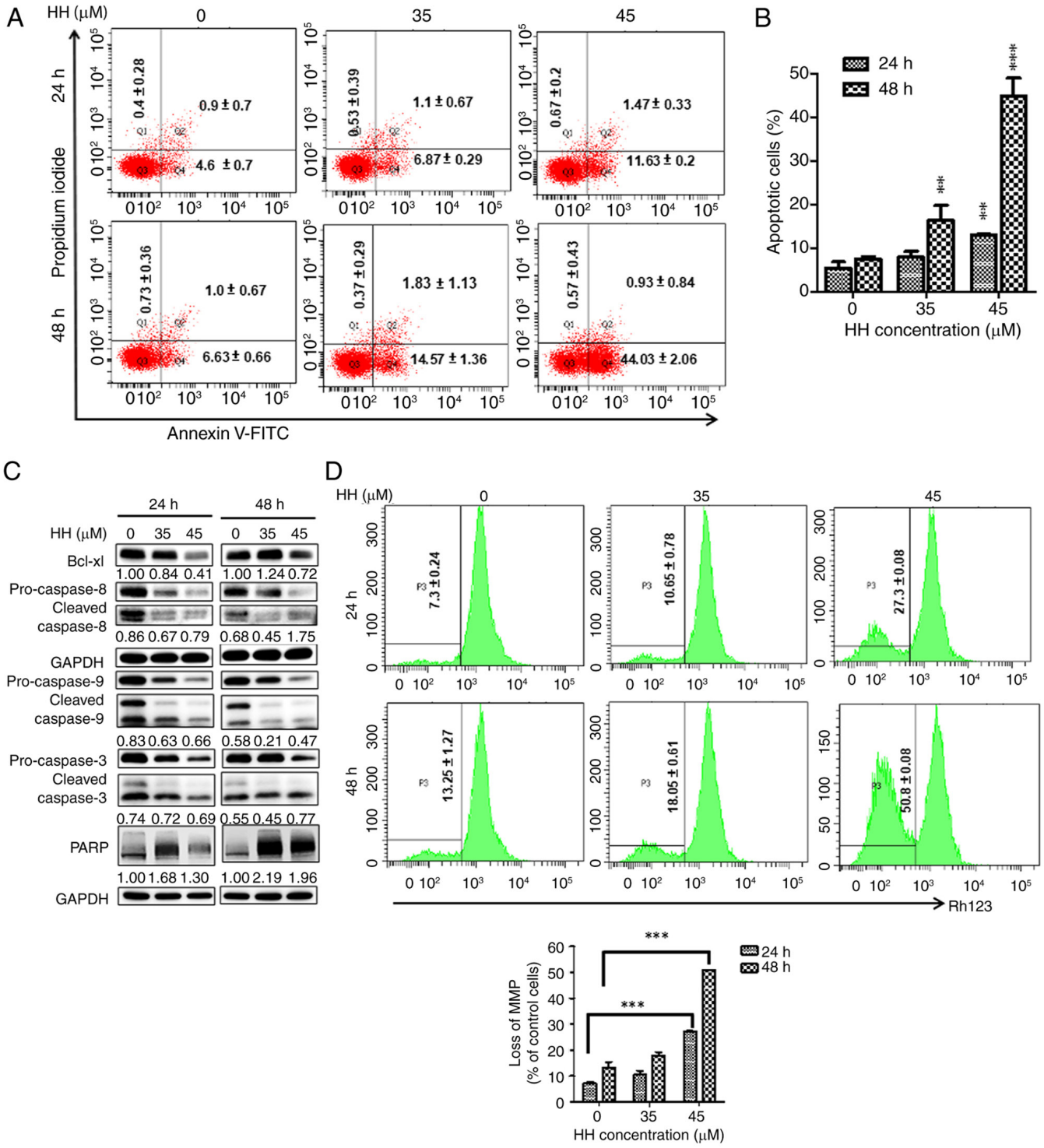

Figure 3. HH increases apoptosis of SCC-4 cells. The lower right quadrant represents early apoptotic cells, indicated as ($FITC^+/PI^-$); the upper right quadrant represents late apoptotic cells, indicated as ($FITC^+/PI^+$); the upper left quadrant represents necrotic cells, indicated as ($FITC^-/PI^+$); and the lower left quadrant represents live cells, indicated as ($FITC^-/PI^-$). The total number of apoptotic cells is the sum of the cells in the lower right and upper right quadrants. (A) SCC-4 cells were treated with HH and apoptotic cells were assessed via flow cytometric analysis. (B) The percentage of apoptotic cells was quantified from three independent experiments. (C) Apoptosis-associated protein expression levels following HH treatment were analyzed using western blotting. (D) MMP was evaluated using flow cytometric analysis in SCC-4 cells following HH treatment. HH 0 μM represents DMSO as the solvent for dissolving HH and serves as the control group. Data are presented as mean ± SD (n=3). **P<0.01, ***P<0.001 vs. control. HH, harmine hydrochloride; MMP, mitochondrial membrane potential; PARP, poly (ADP-ribose) polymerase; Rh123, rhodamine 123.

caspase-3 and PARP (Fig. 5B). Furthermore, comparing HH treatment alone with Z-VAD-FMK pretreatment followed by HH treatment of SCC-4 cells, it was demonstrated that pretreatment with Z-VAD-FMK before HH treatment increased cell viability compared with HH treatment alone (Fig. 5C). Taken together, these findings suggested that HH induced caspase-dependent apoptotic cell death in SCC-4 cells. Caspase activation is also an important factor in

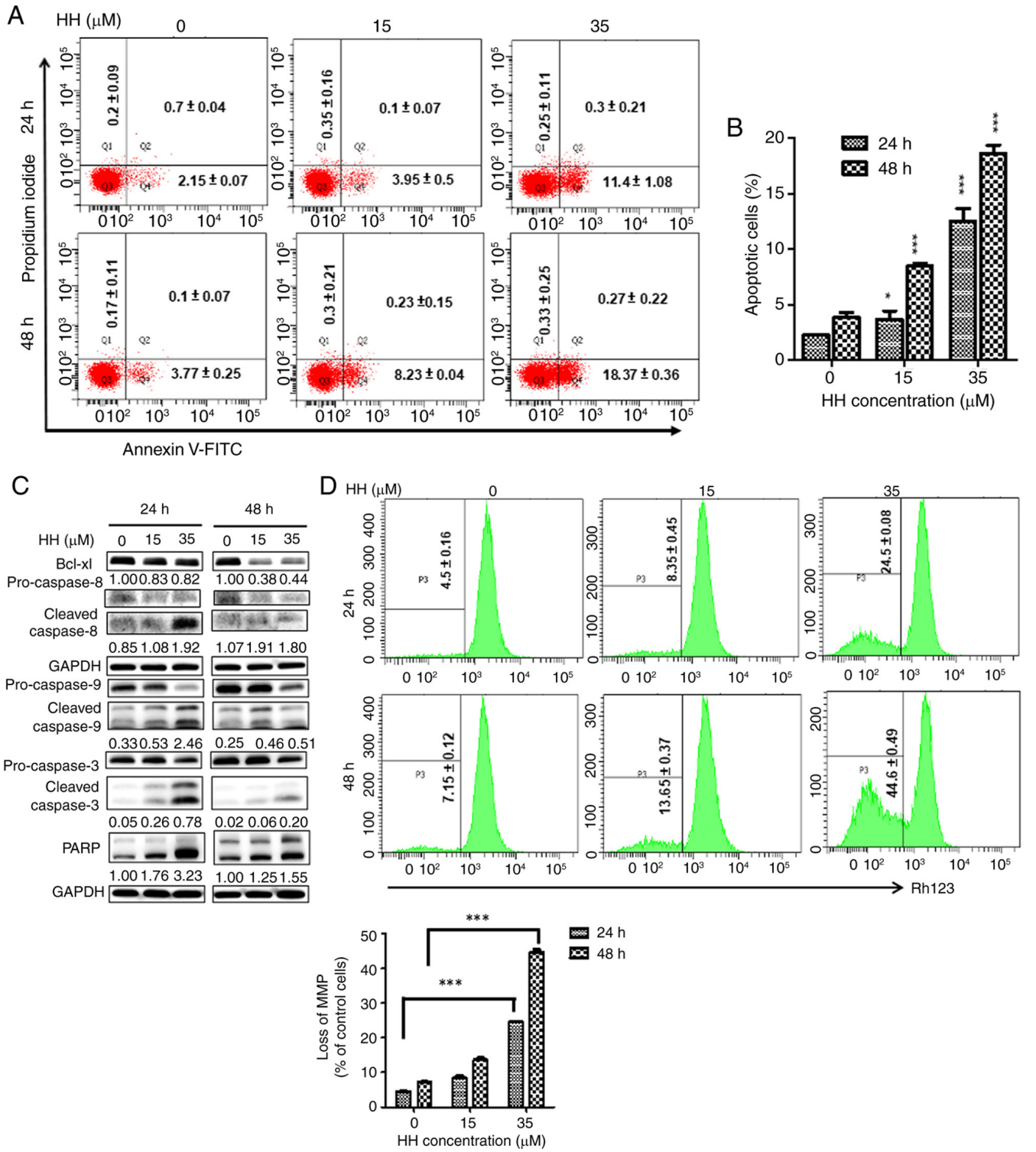

Figure 4. HH increases apoptosis of SCC-25 cells. The lower right quadrant represents early apoptotic cells, indicated as ($FITC^+/PI^-$); the upper right quadrant represents late apoptotic cells, indicated as ($FITC^+/PI^+$); the upper left quadrant represents necrotic cells, indicated as ($FITC^-/PI^+$); and the lower left quadrant represents live cells, indicated as ($FITC^-/PI^-$). The total number of apoptotic cells is the sum of the cells in the lower right and upper right quadrants. (A) SCC-25 cells were treated with HH and apoptotic cells were analyzed using flow cytometry. (B) The percentage of apoptotic cells was determined. (C) Apoptosis-associated protein expression levels following HH treatment were analyzed using western blotting analysis. (D) MMP was analyzed using flow cytometry in SCC-25 cells following HH treatment. HH 0 μM represents DMSO as the solvent for dissolving HH and serves as the control group. Data are presented as mean ± SD (n=3). $^*P<0.01$, $^{***}P<0.001$ vs. control. HH, harmine hydrochloride; MMP, mitochondrial membrane potential; PARP, poly (ADP-ribose) polymerase; Rh123, rhodamine 123.

HH-mediated apoptosis in SCC-25 cells. Although decreases in both the numbers of apoptotic cells (Figs. 5D and S2B) and the protein expression levels of cleaved caspase-3 and PARP in Z-VAD-FMK-pretreated SCC-25 cells compared with the HH-treated SCC-25 cells (Fig. 5E) were observed, by contrast with the results obtained in SCC-4 cells, an increase

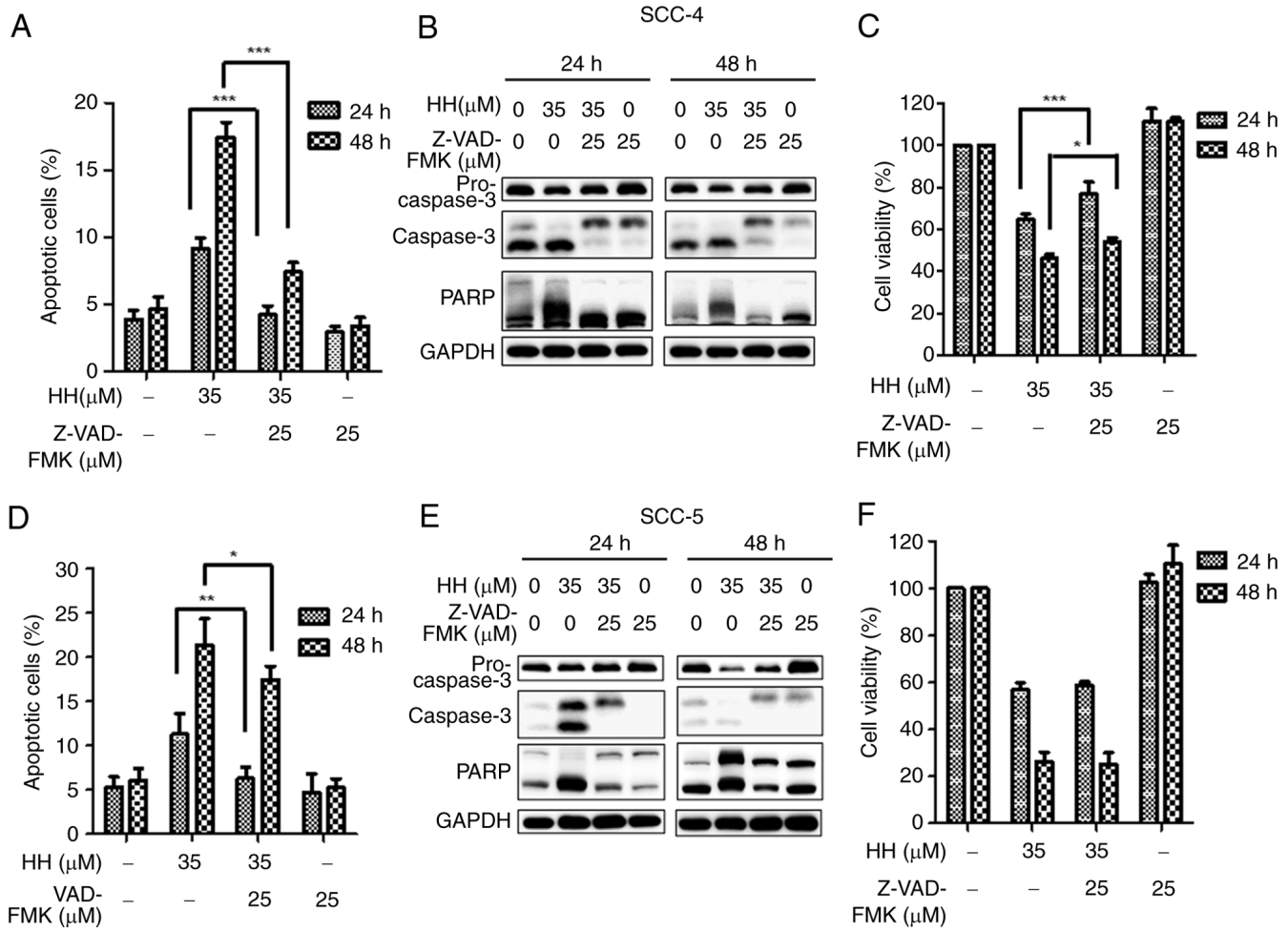

Figure 5. HH-mediated increase in apoptosis HH in oral cancer cells is caspase-dependent. Prior to the application of HH, SCC-4 cells were pretreated with Z-VAD-FMK. (A) The apoptotic cells were subjected to flow cytometric analysis. (B) The expression levels of caspase-3 and PARP proteins were analyzed using western blotting. (C) Cell viability was determined by CCK-8 assay. Before the application of HH, SCC-25 cells were pretreated with Z-VAD-FMK. (D) The apoptotic cells were analyzed using flow cytometric analysis. (E) Western blotting was employed to detect the protein expression levels of caspase-3 and PARP. (F) Cell viability was determined using the CCK-8 assay. HH 0 μM represents DMSO as the solvent for dissolving HH and serves as the control group. Data are presented as mean ± SD (n=3). *P<0.05, **P<0.01, ***P<0.001 vs. control. HH, harmine hydrochloride; CCK-8, Cell Counting Kit-8; PARP, poly (ADP-ribose) polymerase; Z, Z-VAD-FMK; ns, not significant.

in cell viability was not observed in Z-VAD-FMK pretreated SCC-25 cells compared with the HH-treated SCC-25 cells (Fig. 5F). One possibility to account for this result is that SCC-25 cells may be sensitive to the combined treatment of Z-VAD-FMK and HH. In addition, alternative pathways to apoptosis may contribute to HH-induced cell death in SCC-25 cells.

HH induces apoptosis in SCC-4 cells through the MAPK pathway. Given that HH has previously been shown to modulate the MAPK, ERK and JNK signaling pathways in breast cancer and hepatocellular carcinoma cells (29,30), western blotting analysis was performed to investigate which HH target triggered SCC-4 apoptotic cell death. HH treatment was found to activate each of the MAPK, ERK and JNK pathways, as evidenced by the increased expression levels of the respective phosphorylated proteins (Fig. 6A). Furthermore, suppression of ERK and JNK signaling through treatment with the inhibitors PD98059 and SP600125 respectively did not lead to any decrease in the protein expression level of cleaved PARP (Fig. S3); only applying the MAPK pathway inhibitor, SB203580, led to a decrease in the protein expression of cleaved PARP and the apoptotic cell ratio following HH treatment (Fig. 6B and C), suggesting that the MAPK pathway is involved in HH-triggered apoptosis in SCC-4 cells. Taken together, these results suggested that HH triggers SCC-4 cell apoptosis through activating the MAPK pathway.

HH inhibits migration and invasion in OSCC cells. Local invasion is one of the factors that contributes to the poor prognosis of OSCC (31). To evaluate whether HH could inhibit the invasion of OSCC cells, the migratory and invasive capabilities of SCC-4 and SCC-25 cells were assessed following HH treatment. When compared with the control group, HH treatment significantly reduced SCC-4 cell migration in a dose-dependent manner at 24 and 48 h. However, when compared with the control group, only 20 μM HH significantly inhibited invasion, while 10 and 15 μM showed no statistically significant effect at 24 or 48 h after HH treatment (Fig. 7A). A similar trend was observed in the SCC-25 cells; compared with the control group, 5, 10 or 15 μM HH treatment significantly reduced migration by

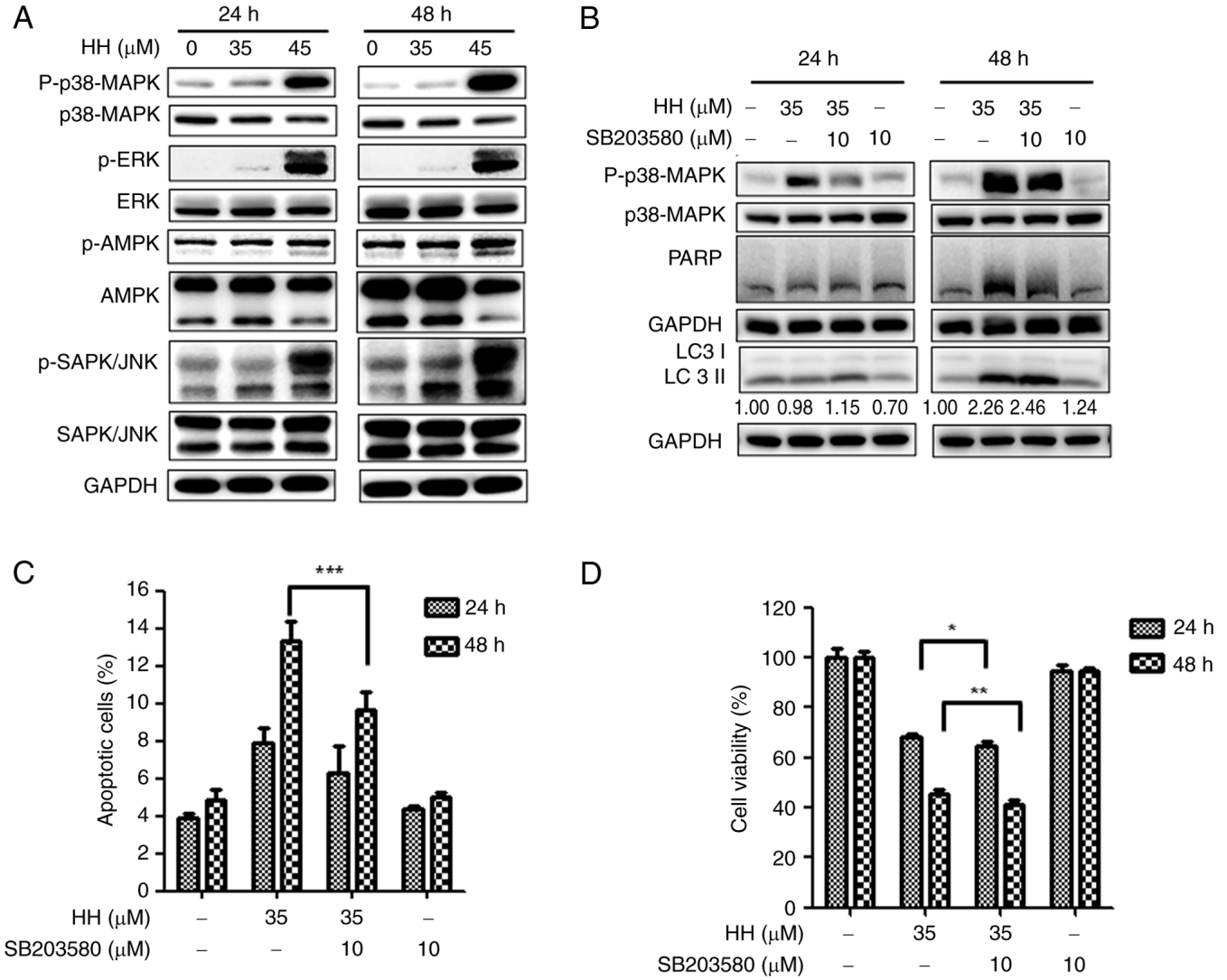

Figure 6. HH-mediated apoptosis in SCC-4 cells is mediated via activation of the MAPK pathway. (A) SCC-4 cells were treated with HH for 24 and 48 h. The protein expression levels of p38, ERK, AMPK and JNK proteins was analyzed by western blotting. (B) SCC-4 cells were pre-incubated with SB203580 prior to HH treatment and the protein expression levels of PARP and LC3 were assessed using western blotting. (C) The ratio of apoptotic cells was determined using flow cytometric analysis. *P<0.05, **P<0.01 and ***P<0.001. HH, harmine hydrochloride; p, phosphorylated.

~20% at 24 h, whereas only 15 μM HH treatment demonstrated a significant effect at 48 h. Compared with the control group, invasion decreased significantly by ~50% in cells treated with 5, 10 or 15 μM HH at both 24 and 48 h. (Fig. 7B). Therefore, the present study demonstrated that HH exhibited cytotoxicity on oral cancer cells and that treatment with HH triggered cell cycle arrest at the G0/G1 phase. It was also demonstrated that activation of the MAPK signaling pathway was involved in HH-induced caspase-dependent apoptosis in SCC-4 cells.

Discussion

Despite improvements in the treatment of oral cancer, including surgical resection combined with radiotherapy or chemotherapy, the morbidity and mortality rates of oral cancer continue to increase worldwide. The annual incidence of this condition has been documented as >377,000 cases and 0.6% increase in mortality globally (1,2). Developing drugs that are derived from natural herbs which may provide reduced side effects is an attractive approach for cancer therapy (32). The present study demonstrated that HH, a derivative of the β-carboline alkaloid harmine, exhibited effective anti-proliferative activity in two OSCC cell lines via G0/G1 cell cycle arrest. Furthermore, the MAPK pathway was demonstrated to be involved in HH-mediated apoptosis in oral cancer cells.

Harmine possesses a diverse range of biological activities; however, its low bioavailability and side effects, such as severe weight loss and acute or delayed locomotor changes in rats, restrict its applicability (16). Therefore, modifications have been made to the β-carboline nucleus of harmine to synthesize derivatives that are lacking these limitations (17). Among these derivatives, HH was synthesized by combining harmine with hydrochloride to enhance its water solubility and bioavailability, and its anti-proliferative activity has been reported in gastric, hepatocarcinoma and colon cancer cells (23,29,33). In cancer cells, HH has been shown to cause cell cycle arrest in the G2/M and the G0/G1 phases. The present study demonstrated that HH caused G0/G1 arrest in both SCC-4 and SCC-25 oral

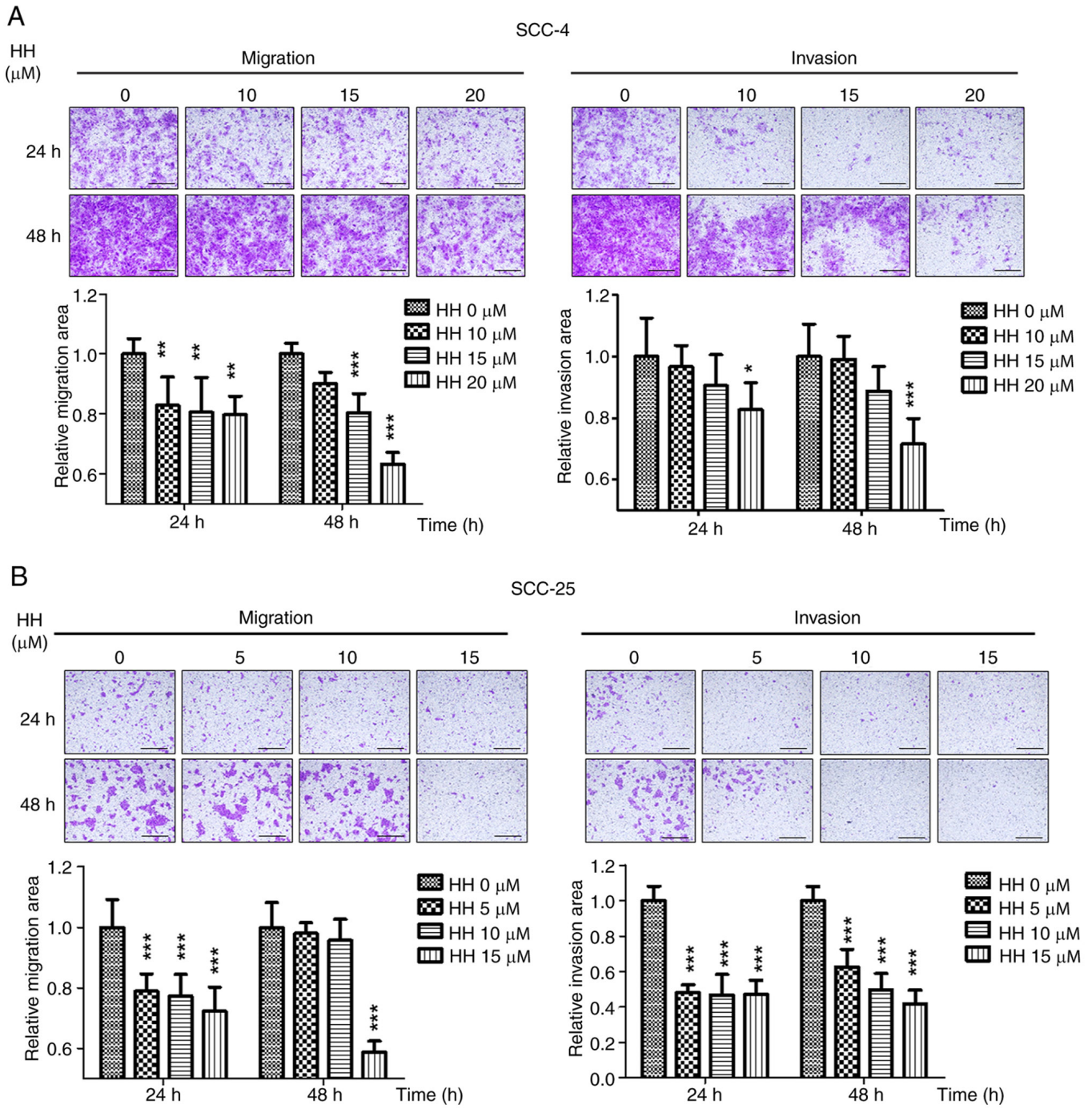

Figure 7. HH inhibits OSCC cells migration and invasion. (A) SCC-4 or (B) SCC-25 cells were seeded onto the upper chamber of the inserts and treated with HH. For the invasion assay, Matrigel was added to the upper chamber. After 24 and 48 h, non-migrated or non-invaded cells were scraped off, and the cells that passed through the insert were stained with crystal violet. The ratio of migration and invasion cells was determined using ImageJ software (version 1.43, National Institutes of Health). Scale bar, 1 mm. HH 0 μM represents DMSO as the solvent for dissolving HH and serves as the control group. *P<0.05, **P<0.01, ***P<0.001 vs. control. HH, harmine hydrochloride.

cancer cells, suggesting that HH may interfere with cell cycle progression at different stages.

Apoptosis induces HH-mediated cell death in cancer cells. Intrinsic or extrinsic pathways activate apoptosis, leading to the activation of caspases (34). Loss of MMP leads to matrix condensation, which subsequently facilitates the release of cytochrome *c*, thereby activating caspases and cell apoptosis (35). Bcl-xL, an anti-apoptotic protein, inhibits apoptosis through impeding the transfer of cytochrome *c* into the cytosol (36). When Bcl-xL is overexpressed, it has a role in both drug resistance and relapse in ovarian cancer and multiple melanoma (37), suggesting that Bcl-xL may be a good target for cancer therapy. In the present study, HH treatment led to decreased protein expression levels of Bcl-xL in SCC-4 and SCC-25 cells. Moreover, flow cytometric analysis results demonstrated a decrease in MMP and an increase of the cleaved forms of caspases-3, -8 and -9. Similarly, HH has been shown to antagonize the effects of Bcl-xL in hepatocarcinoma

and colon cancer cells (22,29,32), suggesting that HH may be a potential anticancer drug for the treatment of oral cancer.

Depending on the cell type and the underlying conditions, such as cell culture passage number, the p38-MAPK signaling pathways respond to stress and are involved in cell survival or apoptosis (38). In the present study, suppression of the MAPK pathways may reduce HH-mediated apoptosis in SCC-4 cells, suggesting that HH-mediated apoptosis occurs through the MAPK pathway in SCC-4 cells. Similarly, HH activates the MAPK pathway to trigger apoptosis in breast and hepatocarcinoma cancer cells (30,32). The MAPK signaling pathway is activated in >50% of the recorded cases of oral cancer (39). Therefore, enhancing MAPK overexpression may be a viable option for treating these types of cancers. However, in SCC-25 cells, the present study did not demonstrate involvement of the MAPK pathway in HH-mediated apoptotic cell death, suggesting that, for this cell line, other signaling pathways may be involved. Further whole genome sequencing may help to identify mechanisms that are associated with HH-mediated cell death. The present study focused solely on the cytotoxic effects of HH on OSCC cells, therefore, performing *in vivo* animal experiments in the future should provide deeper insights into the cytotoxic functions of HH against OSCC. Additionally, synergistic cytotoxic effects between HH and the currently used clinical drugs for OSCC, namely cisplatin and 5-FU, were not observed (data not shown).

In conclusion, the present study demonstrated that HH exerted anti-proliferative activity in oral cancer cells through inducing G0/G1 cell cycle arrest. Furthermore, the MAPK pathway was involved in HH-induced apoptosis in the cell lines tested. These results suggested that HH may have the potential for treating oral cancer in the future.

Acknowledgements

Not applicable.

Funding

The present study was supported by The Ditmanson Medical Foundation Chiayi Christian Hospital (grant no. R110-047).

Availability of data and materials

The data generated in the present study may be requested from the corresponding author.

Authors' contributions

CYF and WTL conceived and designed the experiments. YZL and HYH performed the experiments. PWZ and YNS analyzed the data. CYF and WTL analyzed the data and wrote the manuscript. YZL and CYF confirm the authenticity of all the raw data. All authors read and approved the final version of the manuscript.

Ethics approval and consent to participate

Not applicable.

Patient consent for publication

Not applicable.

Competing interests

The authors declare that they have no competing interests.

References

1. Dong L, Xue L, Cheng W, Tang J, Ran J and Li Y: Comprehensive survival analysis of oral squamous cell carcinoma patients undergoing initial radical surgery. BMC Oral Health 24: 919, 2024.
2. Siegel RL, Giaquinto AN and Jemal A: Cancer statistics, 2024. CA Cancer J Clin 74: 12-49, 2024.
3. Pekarek L, Garrido-Gil MJ, Sánchez-Cendra A, Cassinello J, Pekarek T, Fraile-Martinez O, García-Montero C, Lopez-Gonzalez L, Rios-Parra A, Álvarez-Mon M, *et al*: Emerging histological and serological biomarkers in oral squamous cell carcinoma: Applications in diagnosis, prognosis evaluation and personalized therapeutics (Review). Oncol Rep 50: 213, 2023.
4. Tan Y, Wang Z, Xu M, Li B, Huang Z, Qin S, Nice EC, Tang J and Huang C: Oral squamous cell carcinomas: State of the field and emerging directions. Int J Oral Sci 15: 44, 2023.
5. Deng H, Sambrook PJ and Logan RM: The treatment of oral cancer: An overview for dental professionals. Aust Dent J 56: 244-252, 2011.
6. Eskander A, Dziegielewski PT, Patel MR, Jethwa AR, Pai PS, Silver NL, Sajisevi M, Sanabria A and Doweck I: Oral cavity cancer surgical and nodal management: A review from the american head and neck society. JAMA Otolaryngol Head Neck Surg 150: 172-178, 2024.
7. Fu JY, Yue XH, Dong MJ, Li J and Zhang CP: Assessment of neoadjuvant chemotherapy with docetaxel, cisplatin, and fluorouracil in patients with oral cavity cancer. Cancer Med 12: 2417-2426, 2023.
8. Atashi F, Vahed N, Emamverdizadeh P, Fattahi S and Paya L: Drug resistance against 5-fluorouracil and cisplatin in the treatment of head and neck squamous cell carcinoma: A systematic review. J Dent Res Dent Clin Dent Prospects 15: 219-225, 2021.
9. Jiang Q, Xiao J, Hsieh YC, Kumar NL, Han L, Zou Y and Li H: The role of the PI3K/Akt/mTOR axis in head and neck squamous cell carcinoma. Biomedicines 12: 1610, 2024.
10. Liu L, Chen J, Cai X, Yao Z and Huang J: Progress in targeted therapeutic drugs for oral squamous cell carcinoma. Surg Oncol 31: 90-97, 2019.
11. Xu MJ, Johnson DE and Grandis JR: EGFR-targeted therapies in the post-genomic era. Cancer Metastasis Rev 36: 463-473, 2017.
12. Ferreira DM, Neves TJ, Lima LGCA, Alves FA and Begnami MD: Prognostic implications of the phosphatidylinositol 3-kinase/Akt signaling pathway in oral squamous cell carcinoma: Overexpression of p-mTOR indicates an adverse prognosis. Applied Cancer Research 37: 41, 2017.
13. de Kort WWB, Spelier S, Devriese LA, van Es RJJ and Willems SM: Predictive value of EGFR-PI3K-AKT-mTOR-pathway inhibitor biomarkers for head and neck squamous cell carcinoma: A systematic review. Mol Diagn Ther 25: 123-136, 2021.
14. Satgunaseelan L, Porazinski S, Strbenac D, Istadi A, Willet C, Chew T, Sadsad R, Palme CE, Lee JH, Boyer M, *et al*: Oral squamous cell carcinoma in young patients show higher rates of EGFR amplification: Implications for novel personalized therapy. Front Oncol 11: 750852, 2021.
15. Argiris A, Kotsakis AP, Hoang T, Worden FP, Savvides P, Gibson MK, Gyanchandani R, Blumenschein GR Jr, Chen HX, Grandis JR, *et al*: Cetuximab and bevacizumab: Preclinical data and phase II trial in recurrent or metastatic squamous cell carcinoma of the head and neck. Ann Oncol 24: 220-225, 2013.
16. Chen Q, Chao R, Chen H, Hou X, Yan H, Zhou S, Peng W and Xu A: Antitumor and neurotoxic effects of novel harmine derivatives and structure-activity relationship analysis. Int J Cancer 114: 675-682, 2005.
17. Zhang L, Li D and Yu S: Pharmacological effects of harmine and its derivatives: A review. Arch Pharm Res 43: 1259-1275, 2020.

18. Jalali A, Dabaghian F and Zarshenas MM: Alkaloids of peganum harmala: Anticancer biomarkers with promising outcomes. Curr Pharm Des 27: 185-196, 2021.
19. Hu Y, Yu X, Yang L, Xue G, Wei Q, Han Z and Chen H: Research progress on the antitumor effects of harmine. Front Oncol 14: 1382142, 2024.
20. Tarpley M, Oladapo HO, Strepay D, Caligan TB, Chdid L, Shehata H, Roques JR, Thomas R, Laudeman CP, Onyenwoke RU, *et al*: Identification of harmine and β-carboline analogs from a high-throughput screen of an approved drug collection; profiling as differential inhibitors of DYRK1A and monoamine oxidase A and for in vitro and in vivo anti-cancer studies. Eur J Pharm Sci 162: 105821, 2021.
21. Nafie E, Lolarga J, Lam B, Guo J, Abdollahzadeh E, Rodriguez S, Glackin C and Liu J: Harmine inhibits breast cancer cell migration and invasion by inducing the degradation of Twist1. PLoS One 16: e0247652, 2021.
22. Zhang P, Huang CR, Wang W, Zhang XK, Chen JJ, Wang JJ, Lin C and Jiang JW: Harmine hydrochloride triggers G2 phase arrest and apoptosis in MGC-803 cells and SMMC-7721 cells by upregulating p21, activating caspase-8/Bid, and downregulating ERK/Bad pathway. Phytother Res 30: 31-40, 2016.
23. Tan B, Li Y, Zhao Q, Fan L and Zhang M: The impact of Harmine hydrochloride on growth, apoptosis and migration, invasion of gastric cancer cells. Pathol Res Pract 216: 152995, 2020.
24. Xiong Y, Connolly T, Futcher B and Beach D: Human D-type cyclin. Cell 65: 691-699, 1991.
25. Goel S, Bergholz JS and Zhao JJ: Targeting CDK4 and CDK6 in cancer. Nat Rev Cancer 22: 356-372, 2022.
26. Gudas JM, Payton M, Thukral S, Chen E, Bass M, Robinson MO and Coats S: Cyclin E2, a novel G1 cyclin that binds Cdk2 and is aberrantly expressed in human cancers. Mol Cell Biol 19: 612-622, 1999.
27. Sherr CJ and Roberts JM: Inhibitors of mammalian G1 cyclin-dependent kinases. Genes Dev 9: 1149-1163, 1995.
28. Abukhdeir AM and Park BH: P21 and p27: Roles in carcinogenesis and drug resistance. Expert Rev Mol Med 10: e19, 2008.
29. Kim GD: Harmine hydrochloride triggers G2/M cell cycle arrest and apoptosis in HCT116 cells through ERK and PI3K/AKT/mTOR signaling pathways. Prev Nutr Food Sci 26: 445-452, 2021.
30. Ock CW and Kim GD: Harmine hydrochloride mediates the induction of G2/M Cell cycle arrest in breast cancer cells by regulating the MAPKs and AKT/FOXO3a signaling pathways. Molecules 26: 6714, 2021.
31. Ling Z, Cheng B and Tao X: Epithelial-to-mesenchymal transition in oral squamous cell carcinoma: Challenges and opportunities. Int J Cancer 148: 1548-1561, 2021.
32. Yin SY, Wei WC, Jian FY and Yang NS: Therapeutic applications of herbal medicines for cancer patients. Evid Based Complement Alternat Med 2013: 302426, 2013.
33. Kim GD: Harmine hydrochloride induces G2/M cell cycle arrest and apoptosis in SK-Hep1 hepatocellular carcinoma cells by regulating mitogen-activated protein kinases and the PI3K/AKT pathway. Prev Nutr Food Sci 28: 436-443, 2023.
34. Lossi L: The concept of intrinsic versus extrinsic apoptosis. Biochem J 479: 357-384, 2022.
35. Gottlieb E, Armour SM, Harris MH and Thompson CB: Mitochondrial membrane potential regulates matrix configuration and cytochrome C release during apoptosis. Cell Death Differ 10: 709-717, 2003.
36. Kharbanda S, Pandey P, Schofield L, Israels S, Roncinske R, Yoshida K, Bharti A, Yuan ZM, Saxena S, *et al*: Role for Bcl-xL as an inhibitor of cytosolic cytochrome C accumulation in DNA damage-induced apoptosis. Proc Natl Acad Sci U S A 94: 6939-6942, 1997.
37. Li M, Wang D, He J, Chen L and Li H: Bcl-X(L): A multifunctional anti-apoptotic protein. Pharmacol Res 151: 104547, 2020.
38. Wada T and Penninger JM: Mitogen-activated protein kinases in apoptosis regulation. Oncogene 23: 2838-2849, 2004.
39. Cheng Y, Chen J, Shi Y, Fang X and Tang Z: MAPK signaling pathway in oral squamous cell carcinoma: Biological function and targeted therapy. Cancers (Basel) 14: 4625, 2022.